Study of direct photon production at the CERN LHC

Ashish Kumar, Manoj Kumar Jha, Bani Mitra Sodermark, Ashutosh Bhardwaj, Kirti Ranjan, and R. K. Shivpuri*
Centre for Detector and Related Software Technology, Department of Physics and Astrophysics, University of Delhi, Delhi-110 007, India
(Received 7 October 2002; published 23 January 2003)

Study of direct photon production in high-energy hadronic collisions provides a clean tool for testing the essential validity of perturbative quantum chromodynamics (PQCD) predictions as well as for constraining the gluon distribution of nucleons. These attractive considerations prompted us to study the characteristics of direct photons at CERN LHC energy ($\sqrt{s}=14$ TeV). In order to validate our simulation results, we first describe the direct photon data at $\sqrt{s}=1.8$ TeV in the central pseudorapidity (η) region. We used next-to-leading-order (NLO) QCD calculations and leading-order (LO) PYTHIA estimates with the latest parton distribution function, CTEQ5M1. At $\sqrt{s}=14$ TeV, the LO and NLO QCD predictions for direct photon cross section are presented as a function of transverse momentum of photon (p_T) in the kinematical region 20 GeV$<p_T<$400 GeV and $|\eta|<3$. The sensitivity of the theoretical predictions to the choice of renormalization scales and gluon distributions is also demonstrated. The pseudorapidity (η) and cone size dependence of the direct photon cross section is also discussed.

DOI: 10.1103/PhysRevD.67.014016 PACS number(s): 13.85.Qk, 12.38.Bx, 12.38.Qk

I. INTRODUCTION

Direct (or prompt) photons [1–3] are photons produced directly from the parton-parton interactions [4] and not from secondary decays or as the radiation product of initial or final state partons. These photons emerge unaltered from the hard scattering process and therefore provide a clean probe of the hard-scattering dynamics. This is in marked contrast to the jets-collimated collection of particles arising from the fragmentation of quarks and gluons, since it is generally not possible to precisely and unambiguously define all the remnants of a single quark or gluon. Theoretically, fewer direct photon subprocesses [1] simplifies the situation and the well-understood pointlike coupling of the photon to the quark and gluon makes it easier to perform higher order perturbative quantum chromodynamics (PQCD) calculations. Experimentally, the photons can be clearly identified and their energy and direction can be measured precisely, unlike jets, which are messy due to fragmentation and can only be defined given a certain reconstruction algorithm [2]. Thus the study of large transverse momenta (p_T) direct photons in hadronic collisions serve as an ideal testing ground for the PQCD predictions as it allows an incisive comparison between theory and experiment.

The direct photon cross section is very sensitive to the gluon content of proton because of the dominant contribution from the quark-gluon hard scatterings at the leading-order in proton-proton and proton-antiproton collisions. This is in contrast with deep inelastic scattering (DIS) experiment where the quarks are the major participants and gluons enter only as second order effects. Thus prompt photon cross section constitutes a classical tool for constraining the gluon density [4,5] in conjunction with DIS data.

However, in actual practice, these apparent simplifications must be tempered by having to deal with backgrounds copiously produced from neutral meson decays (especially π^0 and η), a lower event rate compared to jet production, and complications from photons produced during jet fragmentation. Nevertheless, direct photon data provide information which complements that obtained from other hard scattering processes. Furthermore, photons may be important signatures of physics beyond the standard model. Therefore it is necessary to understand the ''conventional'' sources of direct photons before one can fully exploit them in signatures designed to look for new physics.

This analysis describes the study of direct photons in the kinematical regions accessible at CERN LHC energy. After a brief description of the direct photon physics we present the theoretical description of the direct photon data at $\sqrt{s}=1.8$ TeV from the Fermilab Tevatron $p\bar{p}$ collider. Then, we discuss the leading-order (LO) and next-to-leading-order (NLO) predictions for direct photon cross section at $\sqrt{s}=14$ TeV, along with the normalization uncertainty due to the choice of renormalization scale (μ). We show that direct photons can be used to probe gluons at very low values of x and at very high Q^2 by investigating the transverse momentum (p_T) and pseudorapidity (η) distributions of direct photon for different parametrizations of parton distribution functions (PDFs). We have also examined the pseudorapidity interval and cone size dependence of direct photon production. We then discuss background contribution to direct photons due to π^0 decay. As expected, this contribution is seen to overwhelm the prompt γ signal in the lower p_T range. But the signal-to-background ratio improves considerably in the high p_T domain.

II. DIRECT PHOTON SIGNAL

The production of direct photons at the Born level, $O(\alpha\alpha_s)$, proceeds primarily through quark-gluon Compton scattering $qg\rightarrow q\gamma$ and quark-antiquark annihilation scattering $q\bar{q}\rightarrow g\gamma$, [1,2] as shown in Fig. 1(a). The characteristic feature of both of the subprocesses is that the high p_T direct

*Corresponding author. Email address: hep@nda.vsnl.net.in, cdrst@hepdelhi.com

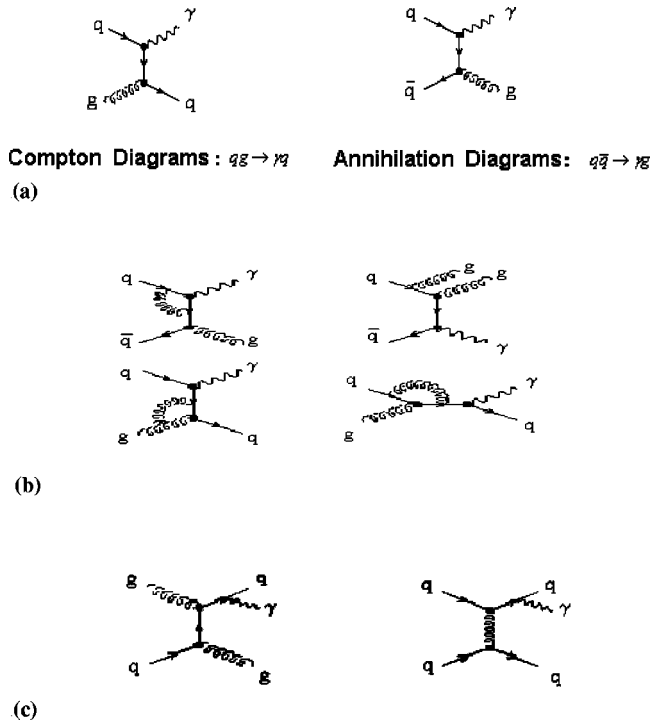

FIG. 1. Direct photon subprocesses: (a) The leading order (LO) diagrams, (b) a few next-to-leading-order (NLO) diagrams, and (c) anomalous (bremsstrahlung) processes.

photon is well isolated from the other hadrons in the event and it recoils against a balancing high p_T jet resulting from quark or gluon fragmentation which appears on the opposite side of the event. The Compton scattering is directly sensitive to the gluon density of the proton [4], the recoil jet is usually a *u* quark. The annihilation mechanism, if isolated, enables the recoil gluon jet to be studied in relation to the quark jet [4]. Because of the abundance of low momentum fraction (*x*) gluons in the proton, Compton scattering is the dominant QCD mechanism contributing to prompt photon production over most of the kinematical region in proton-proton collisions as well as for low to moderate values of parton momentum fraction *x* in proton-antiproton collisions. This can be understood from the sharply peaked gluon distribution in the low-*x* domain and the very fast decrease as compared to quark distribution in the high-*x* region. The annihilation process provides very meager contribution, but gains more and more importance with increasing *x* in $p\bar{p}$ collisions. At higher energies, larger momentum quarks are necessary to produce such an energetic photon and so the annihilation diagram becomes more prominent. In proton-antiproton interactions, the photon cross section is enhanced by the relatively more significant contribution from annihilation scattering (because of the greater availability of the valence antiquark), which gains over the Compton process at high-*x* values.

A few higher order subprocesses, which contribute to the direct photon production, are shown in Fig. 1(b). These are the processes with extra gluons radiated from initial or final-state partons, or processes with gluon loops as correction to the original leading order processes. The characteristic experimental signature is a photon plus two or more jets. Current NLO PQCD calculation only go up to the two jet level, $O(\alpha\alpha_s^2)$, the next-to-leading-order (NLO) terms.

A. Anomalous (bremsstrahlung) component

In addition to the direct production of photons, there are various processes, which involve the radiation of fairly high p_T photons from final state quarks in a dijet event, called bremsstrahlung processes [Fig. 1(c)] [6,7]. These are not considered to be prompt photons as they are not produced directly from the hard interaction vertex, but the existence of this production mechanism affects the way in which direct photons are measured and modeled theoretically.

Because the bremsstrahlung photons tend to be collinear with the quark, and therefore the jet, from which it is radiated, an isolation criterion is used routinely in the collider regime to suppress such events. This method is based on the expectation that direct photons are fairly isolated in the detector while photons from anomalous contributions usually have quite a few hadrons in their vicinity coming from fragmentation products of the outgoing parton. The isolation requirement is typically implemented by measuring the amount of energy in the calorimeter inside a cone of radius *R* (typically $R=0.4$–1.0) centred on the photon candidate and requiring that the hadronic energy be smaller than a certain amount. This strongly discriminates against production of photons from the bremsstrahlung process, but the backgrounds that mimic this process are too large to allow a direct measurement. This requirement, unfortunately, can do nothing to remove bremsstrahlung photons that are radiated at large angles with respect to jets. Such an isolation cut suppresses but does not totally remove this component. Theoretical calculations involve the nonperturbative fragmentation functions to account for bremsstrahlung contribution, which is partially removed by the isolation cut matching that of the experiment. At first guess, one might expect that bremsstrahlung (e.g., $qq \to qq\gamma$ or $qg \to qg\gamma$, etc.) could be of the order $O(\alpha\alpha_s^2)$ and perhaps negligible in most regions of phase space. This, however, is not the case entirely because the fragmentation function of a constituent into a photon scales as α/α_s and the cross section for the bremsstrahlung component is of the same order $O(\alpha\alpha_s)$ [6,7] as the two leading order fundamental QCD subprocesses.

B. Background events

The experimental candidate photon samples are always contaminated by substantial backgrounds, which greatly complicate the analysis of the direct photon signal. The dominant background to the prompt photon events comes from jets. While most jets consist of many particles, and are thus easily distinguishable from a single photon, a small fraction (one in 10^3 to 10^4) fragments in such a way that a single particle gains most of the energy of the parent parton. If that particle is a neutral meson, like π^0 or η that can decay to two photons, the decay product may be indistinguishable from a single photon since at high energies the two photon showers coalesce into a single cluster in the calorimeter. The isolation criteria rejects the bulk of these jets leaving about

0.1% of them which fragment this way and mimic a true photon signal. While only one in 10^3 to 10^4 jets fragments this way, the dijet cross section is 10^3 to 10^4 times larger than that of the photon cross section. Therefore the rate at which single particle jets are produced is similar to the rate at which prompt photons are produced, thus contributing to a severe background to the direct photon sample. It is therefore very important to understand the background evaluation and extraction as precisely as possible. Its precise knowledge is also crucial to pin down the existence of new particles such as $H\rightarrow\gamma\gamma$ or any breaking down of symmetry in the standard model. The decay of π^0 mesons into two photons forms the largest contribution [8,9] to the background since π^0's are most commonly produced. The amount of background depends on the granularity of the calorimeter and on the strategies adopted to reconstruct the showers. At collider energies, it is very important in the low p_T region but the signal-to-background ratio is enhanced as p_T increases [8,9].

III. THEORETICAL FORMALISM

In the framework of QCD perturbation theory, the differential cross section for the inclusive single prompt photon production, $h_1h_2\rightarrow\gamma X$, in transverse momentum (p_T) and pseudorapidity (η) can be written in a factorized form as

$$\frac{d\sigma}{dp_T d\eta}=\frac{d\sigma^{dir}}{dp_T d\eta}+\frac{d\sigma^{brem}}{dp_T d\eta}, \tag{1}$$

where we have distinguished the ''direct'' component (σ^{dir}) from the ''bremsstrahlung'' one (σ^{brem}). Each of these terms is known in the next-to-leading logarithm approximation in QCD, i.e., we have

$$\frac{d\sigma^{dir}}{dp_T d\eta}=\sum_{i,j=q,g}\int dx_1 dx_2 F_{i/h_1}(x_1,M)F_{j/h_2}(x_2,M)\times\frac{\alpha_s(\mu)}{2\pi}\left\{\frac{d\widehat{\sigma_{ij}}}{dp_T d\eta}+\frac{\alpha_s(\mu)}{2\pi}K_{ij}^{dir}(\mu,M,M_F)\right\} \tag{2}$$

and

$$\frac{d\sigma^{brem}}{dp_T d\eta}=\sum_{i,j,k=q,g}\int dx_1 dx_2\frac{dz}{z^2}F_{i/h_1}(x_1,M)F_{j/h_2}(x_2,M)\times D_{\gamma/k}(z,M_F)\frac{\alpha_s(\mu)}{2\pi}\left\{\frac{d\sigma_{ij}{}^{k}}{dp_T d\eta}+\frac{\alpha_s(\mu)}{2\pi}K_{ij,k}^{brem}(\mu,M,M_F)\right\}, \tag{3}$$

where the parton densities in the initial hadrons (F_{i/h_1} and F_{j/h_2}) and the parton to photon fragmentation function ($D_{\gamma/k}$) have been convoluted with the partonic cross sections of the hard scattering subprocesses, x being the parton's momentum fraction and z being the longitudinal momentum fraction of parent parton carried by the bremsstrahlung photon. Here we have neglected the transverse motion of partons (k_T) prior to hard scattering. The higher order correction terms to the direct and bremsstrahlung cross sections are represented by K_{ij}^{dir} [10,11] and $K_{ij,k}^{brem}$ [12], respectively. The parton distribution functions [13–15] and fragmentation functions [16,17] are extracted via global analysis of experimental data particularly from deep inelastic lepton-proton scattering.

A. Scale sensitivity

The intrinsic uncertainties of the NLO QCD predictions are related to the choice of three arbitrary scales: the renormalization scale μ which appears in the evolution of strong coupling constant α_s, the factorization scale M associated to the initial state collinear singularities, and the fragmentation scale M_F related to the collinear fragmentation of a parton into a photon. Roughly speaking, these are the parameters which control how much of the higher effects are resummed in $\alpha_s(\mu)$, $F_{i/h}$, and $D_{\gamma/k}$, respectively, and how much is treated perturbatively in K_{ij}^{dir} and $K_{ij,k}^{brem}$. As these scales are unphysical, the theory can be considered reliable only in the region of the phase space where the predictions are stable with respect to the scale variations [18]. At the leading logarithm level, the photon cross section depends sensitively on the specific choice used for scales. When the next-to-leading logarithm terms are included, it makes the theory more complete and less sensitive to the choice of scales. Current NLO QCD calculations for direct photon cross section have been performed both analytically [19–26] and in Monte Carlo framework [27,28] which conventionally choose all three scales to be equal to the photon transverse momentum p_T.

B. Pseudorapidity dependence

Previous theoretical analysis [6] has shown that the direct photon cross section has a pseudorapidity (η) dependence which is sensitive to the parametrization of the gluon distribution functions. This sensitivity is even more dramatic in the lower transverse momentum or in the forward regions of the detector. Since earlier direct photon experiments with the exception of DZERO and Collider Detector at Fermilab (CDF) have concentrated on the central region, the forward direct photon detection capability of the CMS detector ($\eta<2.5$) at CERN Large Hadron Collider (LHC) allows us a new kinematical region for investigating the pseudorapidity dependence where the gluon distribution within hadrons can be constrained. This motivation is based on the fact that the transverse momentum fraction probed by the photons is

$$x_T=\frac{2p_T}{\sqrt{s}}$$

which is related to the momentum fraction of the partons x as $\hat{s}=x_1x_2s$. If the initial partons are of nearly equal momenta, the photon-jet system will retain its center-of-mass back-to-back nature in the laboratory frame. Then in the central region $\eta=0$, $x_T=x$. Now, if one parton is of much greater momentum than the other, then the system is boosted as the

TABLE I. The variation in $x_{g(min)}$ with changes in p_T cuts and η values at LHC.

p_T (GeV/c)	x_T	$x_{g(min)}$ $\eta=0.5$	$x_{g(min)}$ $\eta=1.0$	$x_{g(min)}$ $\eta=1.5$	$x_{g(min)}$ $\eta=2.0$	$x_{g(min)}$ $\eta=2.5$	$x_{g(min)}$ $\eta=3.0$
20	0.0029	8.7×10^{-4}	5.3×10^{-4}	3.2×10^{-4}	2.0×10^{-4}	1.2×10^{-4}	7.3×10^{-4}
50	0.0071	2.2×10^{-3}	1.3×10^{-3}	8.0×10^{-4}	5.0×10^{-4}	3.1×10^{-4}	1.9×10^{-4}
100	0.0142	4.4×10^{-3}	2.7×10^{-3}	1.6×10^{-3}	1.0×10^{-3}	6.4×10^{-4}	4.2×10^{-4}
150	0.0214	6.6×10^{-3}	4.1×10^{-3}	2.4×10^{-3}	1.6×10^{-3}	1.0×10^{-3}	6.8×10^{-4}
200	0.0286	8.9×10^{-3}	5.5×10^{-3}	3.3×10^{-3}	2.2×10^{-3}	1.4×10^{-3}	1.0×10^{-3}
250	0.0357	1.1×10^{-2}	6.9×10^{-3}	4.1×10^{-3}	2.8×10^{-3}	1.9×10^{-3}	1.3×10^{-3}
300	0.0429	1.3×10^{-2}	8.4×10^{-3}	4.9×10^{-3}	3.4×10^{-3}	2.4×10^{-3}	1.9×10^{-3}
350	0.0500	1.6×10^{-2}	9.9×10^{-3}	5.8×10^{-3}	4.1×10^{-3}	3.0×10^{-3}	2.5×10^{-3}
400	0.0571	1.8×10^{-2}	1.1×10^{-2}	6.7×10^{-3}	4.9×10^{-3}	3.6×10^{-3}	3.3×10^{-3}

more energetic parton overwhelms the softer ones, and the final state objects tend to be on the same side of the event. Since gluons typically carry much less of the momentum of the proton than do quarks, i.e., $x_g \ll x_q$, one expects that in direct photon production large momentum imbalances will dominate, and the final state will tend to be boosted in the direction of the incoming quark. In other words, both the photon and the jet will tend to be produced at small angles, either both forward ($\eta>0$) or both backward. The minimum momentum fraction of the hard scattering partons probed by the inclusive measurements is roughly

$$x_{min}=\frac{x_T e^{-\eta}}{2-x_T e^{\eta}},$$

and larger values of η correspond to smaller values of x_{min} where the gluon distribution is peaked [30] which means that high η photons are more likely to have come from gluon interactions. As one goes to lower p_T or higher η, there is an increased contribution from gluons near the x range around 10^{-4} to 10^{-3} where they are dominant in hadronic structures [1,29]. The LHC will open up a new kinematic region which will give the opportunity to study gluons of low x at higher Q^2 than at HERA. Table I gives the value of $x_{g(min)}$ for different kinematical cuts at LHC.

IV. MONTE CARLO SIMULATION

A Monte Carlo (MC) simulation based on PYTHIA 6.2 code [30] is used to calculate the direct photon cross section by generating $10^5 pp$ events at center-of mass energy of 14 TeV. The parton level subprocesses employed to simulate γ-jet events were $qg\rightarrow q\gamma$, $q\bar{q}\rightarrow g\gamma$, and $gg\rightarrow g\gamma$. PYTHIA describes the hard scattering between hadrons via leading-order perturbative QCD matrix elements. PYTHIA was also used to generate the background contribution due to π^0 decay.

V. DIRECT PHOTON PRODUCTION AT TEVATRON

In Fig. 2(a) we compare the measurement of the differential cross section for production of isolated prompt photons in proton-antiproton collisions at Tevatron ($\sqrt{s}=1.8$ TeV) by CDF Collaboration during run 1B [31] with the corresponding theoretical calculations. The leading-order (LO) QCD calculations are generated by simulating the direct photon events using PYTHIA with the latest parton distribution function (PDF), CTEQ5M1, and the renormalization scale $\mu=p_T$. The next-to-leading-order (NLO) PQCD calculations [27,42] are those provided by Vogelsang [32] and are derived using the CTEQ5M1 parton distribution function (PDF) [33] with the renormalization, factorization, and fragmentation

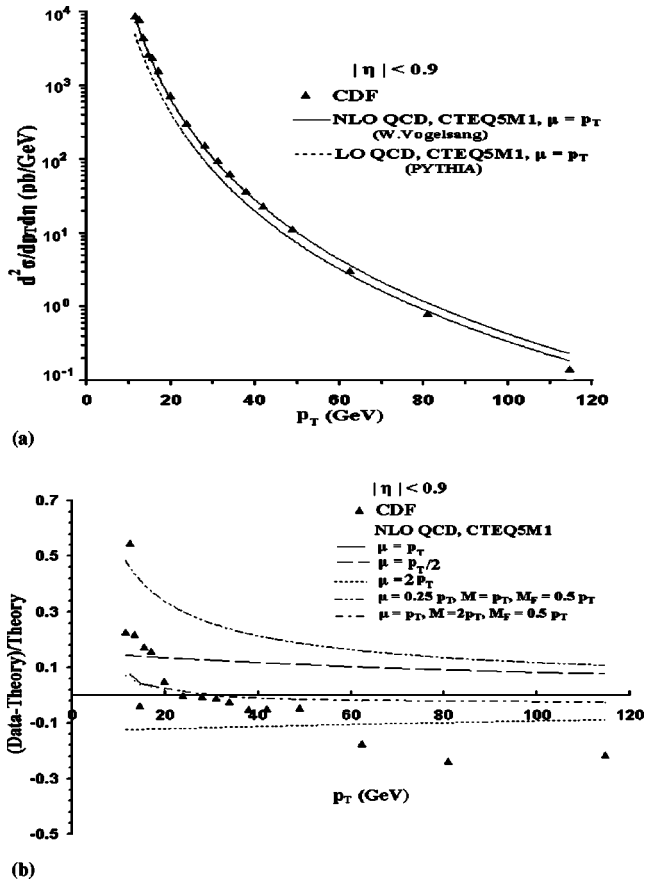

FIG. 2. Tevatron data analysis: (a) A comparison of the 1.8 TeV data from CDF to a NLO QCD calculation as a function of p_T, and (b) comparison of CDF data at 1.8 TeV with NLO theory for a different choice of scales.

scales set at p_T. This calculation imposes an isolation criterion, which rejects events with a jet of $E_T > 1$ GeV in a cone of radius 0.4 around the photon.

We see that the expectations from LO disagree with the data and the NLO QCD predictions agree qualitatively with the measurements over a wide range of p_T. The visual comparison between data and theory is aided by plotting (data $-$theory)/theory on a linear scale [Fig. 2(b)] which shows that the shape of the measured cross sections versus p_T is generally steeper than that of theoretical predictions. There is a general agreement between data and theory in the intermediate region (25 GeV$< p_T <$60 GeV) but a striking excess at low p_T ($<$25 GeV/c) by at most 56% and a deficit of around 22% in the high p_T region.

The change of renormalization scale from $\mu = p_T$ to $\mu = p_T/2$ or $\mu = 2p_T$ changes the predicted cross sections by $<$10% thus producing a small normalization shift throughout with no change in slope. Simultaneous variations of all the theoretical scales (renormalization scale μ, factorization scale M, and fragmentation scale M_F) [34] independently also produces a small change in the shape of the predictions, but does not reproduce the shape of measured cross sections, as can be seen from Fig. 2(b). However, one should not worry too much about the large p_T regime keeping in mind that data have a 14% normalization uncertainty, and that changing scales in the theory also produces roughly that sort of uncertainty in normalization. The low p_T excess of data over theory is consistent with previous observations [9,35] at collider and fixed-target energies. This excess may originate in additional multiple soft-gluon radiations (which could give a recoil effect to the photon+jet system) [36–38] beyond that included in the QCD calculations, or reflect inadequacies in the parton distribution functions [39] and fragmentation contributions. It has been suggested [36–38] that the smearing of transverse momentum of initial state partons (k_T kick) can probably explain this low p_T discrepancy since any uniform smearing on a steeply falling distribution enhances significantly only the low p_T end of the spectrum. Higher order QCD calculations including soft-gluon effects through the resummation technique are becoming available [40,41] but are not currently ready for detailed comparisons.

VI. EXPECTATIONS FOR DIRECT PHOTONS AT LHC

A. Leading-order (LO) cross section

Figure 3(a) shows the transverse momentum (p_T) distribution of a LO inclusive cross section for direct photon production at LHC in the kinematical range 20 GeV$< p_T <$400 GeV and pseudorapidity interval $|\eta| < 3$. Also displayed are the contributions from the various parton scattering subprocesses. For ease of comparison, the same results are shown in Fig. 3(b) on a linear scale relative to the total rate. The results in both of these figures were generated using the leading-logarithm approximation by simulating direct photon events using PYTHIA with the CTEQ5M1 parton distribution function and with the renormalization scale $\mu = p_T$. The results shown in Figs. 3(a) and 3(b) reveal that the Compton scattering provides the dominant mode of direct photon production in the entire kinematical region which is indicative of the fact that the direct photon data from LHC would provide constraints on the gluon distribution in global fits of parton distributions in the high-x_T ($=2p_T/\sqrt{s}$) range. The annihilation scattering provides relatively small contribution in the low and intermediate regions, but its contribution becomes more and more significant with increase in p_T. Also, the gluon-gluon initiated processes are not expected to play a significant role over the p_T range shown.

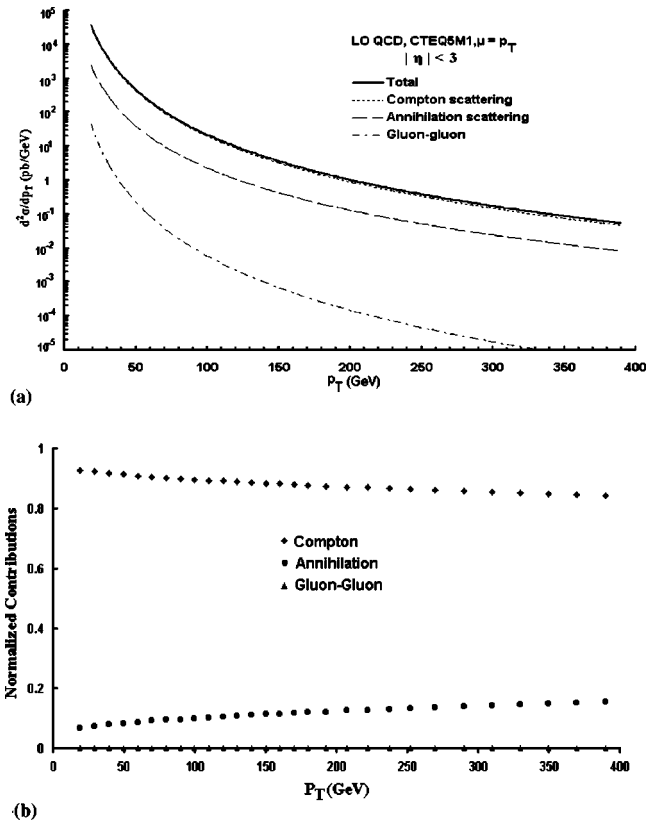

FIG. 3. Inclusive direct photon cross section to leading order at LHC energy: (a) Contributions of various parton level subprocesses, and (b) the same results as shown above except on a linear scale and normalized to the total rate at each value of p_T.

B. Next-to-leading-order (NLO) cross section

Figure 4(a) plots the spectrum of NLO QCD predictions [27] for direct photon cross section at LHC along with the LO (PYTHIA) estimates, evaluated with the CTEQ5M1 parton distribution function and renormalization scale $\mu = p_T$ in the same pseudorapidity interval $-3 < \eta < 3$. The NLO calculations [27,42] are those provided by Vogelsang [32] and use the same isolation cut as that of CDF run IB. In comparison to the cross section at Tevatron energy (Fig. 4), this distribution extends to greater than three times than at the Tevatron. We see that the NLO QCD contribution is higher than the LO in the whole p_T range under analysis.

C. *K*-factor

All PYTHIA cross-section estimates are based primarily on leading-order (LO) calculations. Often these LO cross sec-

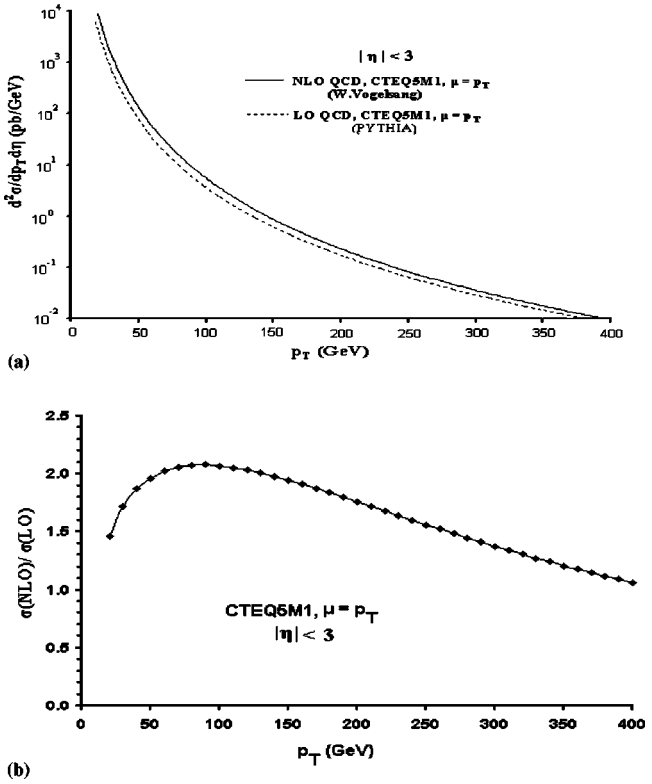

FIG. 4. (a) LO and NLO QCD predictions for direct photon cross section at LHC. (b) Variation of relative contributions of LO and NLO terms as a function of p_T.

tions $[\sigma(\mathrm{LO})]$ differ significantly from the theoretical next-to-leading-order QCD $[\sigma(\mathrm{NLO})]$ calculations. The ratio of $[\sigma(\mathrm{NLO})]/[\sigma(\mathrm{LO})]$ defines the so-called *K*-factor. Figure 4(b) shows how the NLO results of direct photon cross section at the LHC differ from the LO cross section as a function of p_T. Numerical PYTHIA "*K*-factors" [42] are derived for three PDF's. *K*-factors of up to 2 have been plotted for CTEQ5M1 in Fig. 4(b). We see that NLO contribution to the cross section decreases with rise in p_T. This is mainly due to a considerable decrease in the higher-order soft-gluon corrections as p_T increases.

D. Scale dependence of inclusive cross sections

To see the renormalization scale (μ) dependence of the theoretical predictions for direct photon inclusive cross section we compare the LO and NLO QCD results with CTEQ5M1 parton distribution function in the central rapidity region, $y=0$, for scales $\mu=p_T/2$ and $\mu=2p_T$ normalized to the conventional scale $\mu=p_T$ in Fig. 5. We see that the LO calculations show strong scale dependence at low p_T. At $p_T=20$ GeV, the variation of scale between $p_T/2$ and $2p_T$ leads to a normalization uncertainty of around 25%. Again, the scale dependence gains more and more significance in the high p_T region and at $p_T=400$ GeV, the variation of scale between the above limits changes the cross section by around 25%. This variation of LO QCD calculations with scale implies the need for incorporating higher order correction factors. As expected, we notice from Fig. 5 that the

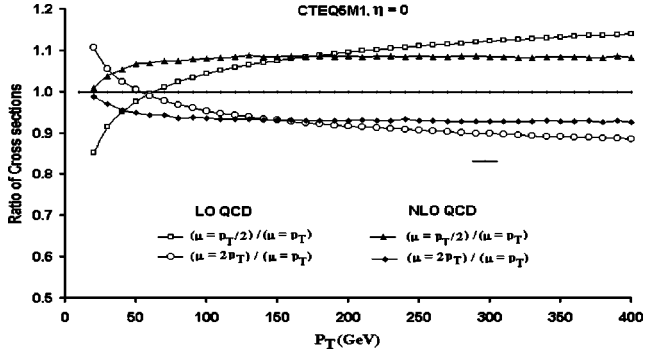

FIG. 5. Ratio of LO and NLO QCD cross sections for direct photons at LHC for different choices of μ ($\mu=p_T/2$ and $\mu=2p_T$) normalized to that for conventional choice $\mu=p_T$.

NLO QCD calculations are less sensitive to the choice of scale. The variation of scale between $p_T/2$ and $2p_T$ leads to a normalization uncertainty of at most 14% over the whole range under consideration, thus showing the reliability of perturbative QCD predictions.

E. Sensitivity to gluon distributions

1. The p_T spectrum

As an illustration of sensitivity of direct photon production to the different parametrizations of gluon distribution, we compare the spectrum of NLO QCD predictions for direct photon cross section averaged in the pseudorapidity region $|\eta|<3$ due to different choices of parton distribution functions (PDFs). The PDFs are CTEQ3M, CTEQ4M, CTEQ5M, CTEQ5Hj [43–45], MRS99 [14], and GRV 94M [46] which are normalized to that of CTEQ5M1 PDF (Fig. 6). In general, theoretical uncertainties are greatly reduced due to the ratio of cross sections. As can be seen from Fig. 6, the ratio of cross sections is almost insensitive to the choice of PDF at high $p_T>300$ GeV, corresponding to $x_T>0.05$, but exhibits more and more sensitivity as we move to the low p_T region. The ratio of the recent PDFs (CTEQ5M, CTEQ5Hj) and CTEQ5M1 is consistent with unity within at most 4% excess over the range under consideration. The

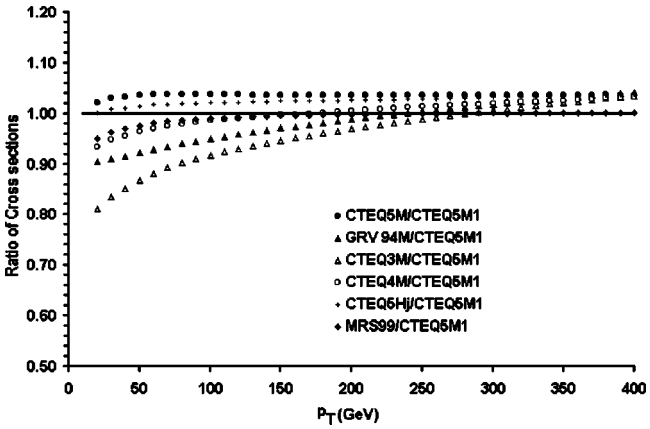

FIG. 6. Transverse momentum (p_T) spectra of direct photon cross section at LHC for different parton distribution functions.

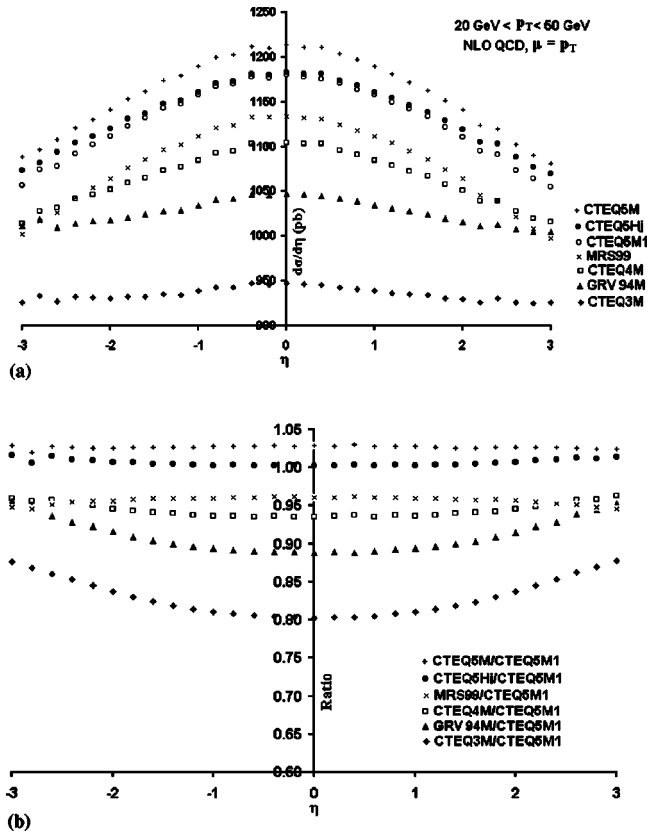

FIG. 7. (a) Pseudorapidity (η) spectra of direct photon cross section at LHC for different PDFs integrated over 20 GeV/c $<p_T<$ 50 GeV/c. (b) The η spectra of the ratio of cross sections for different PDFs normalized to that of CTEQ5M1 for 20 GeV/c $<p_T<$ 50 GeV/c.

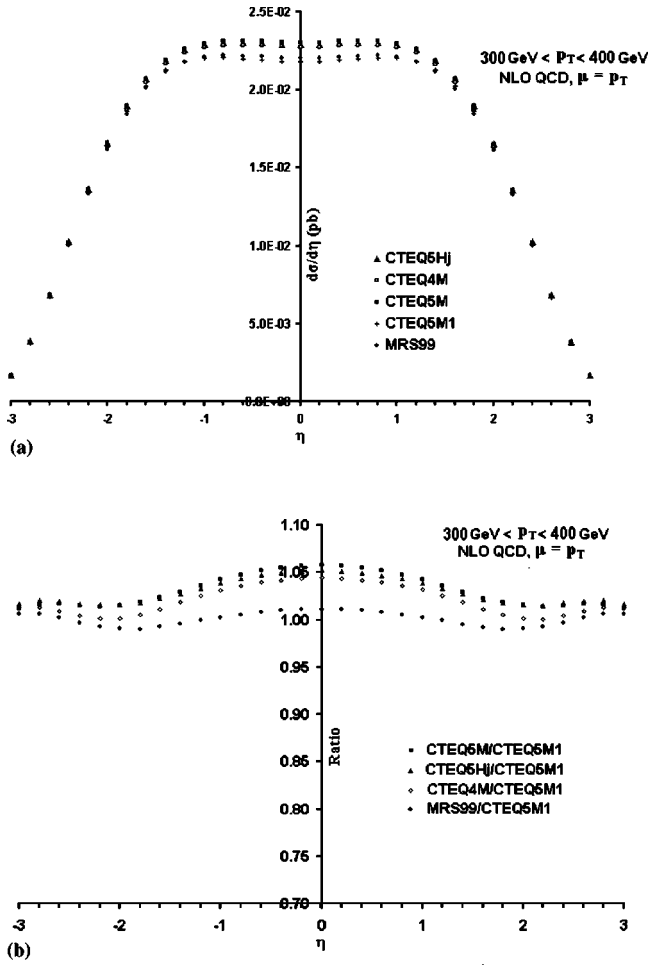

FIG. 8. (a) Pseudorapidity (η) spectra of direct photon cross section at LHC for different PDFs integrated over 300 GeV/c $<p_T<$ 400 GeV/c. (b) The η spectra of the ratio of cross sections for different PDFs normalized to that of CTEQ5M1 for 300 GeV/$c<p_T<$ 400 GeV/c.

MRS99 PDF coincides with the CTEQ5M1 at high p_T and shows a deficit at low p_T of at most 5%. GRV94M and CTEQ3M are significantly lower at low p_T by at most 10% and 20%, respectively. Thus we notice that the spectrum of prompt photons is slightly sensitive to the small-x behavior of gluon distribution.

2. The η spectrum

a. Low p_T region. Figure 7(a) shows the pseudorapidity distribution of a NLO QCD cross section for direct photons with their transverse momenta, 20 GeV$<p_T<$50 GeV, for different parton distribution functions. We note that production of photons is fairly high in the central rapidity region. We also see that η spectrum is quite sensitive to the parton distribution function, particularly in the central region. This is more explicitly exhibited from the spectrum of the ratio of cross section for different PDFs normalized to that of CTEQ5M1 [Fig. 7(b)]. Thus η spectrum of direct photons is more helpful in obtaining information about the gluon distribution for small-x gluons.

b. High p_T region. Figure 8(a) shows the pseudorapidity distribution of NLO QCD predictions for a direct photon cross section with different PDFs for high transverse momentum of photons, 300 GeV$<p_T<$400 GeV. We see that from the η spectrum of direct photons it is very difficult to distinguish between the different parametrizations of the gluon distribution. This is also illustrated from the η spectrum of ratio of cross section with different PDFs normalized to that of CTEQ5M1 [Fig. 8(b)]. Thus the η distribution of the direct photon cross section is almost insensitive to the large-x behavior of gluons.

F. Pseudorapidity dependence

Figures 9(a) and 9(b) show the distributions of LO and NLO QCD predictions for an integrated direct photon cross section in different pseudorapidity windows. As expected, cross section is more for larger η interval. Figure 9(c) compares the averaged differential cross sections for direct photons in different pseudorapidity bins normalized to the cross section for $\eta=0$. We see that direct photons are produced fairly copiously in the central region. The production rate decreases in the high η domain, particularly at high p_T.

G. Cone size dependence

Figure 10(a) illustrates the cone size dependence of the NLO QCD predictions for a direct photon cross section as a

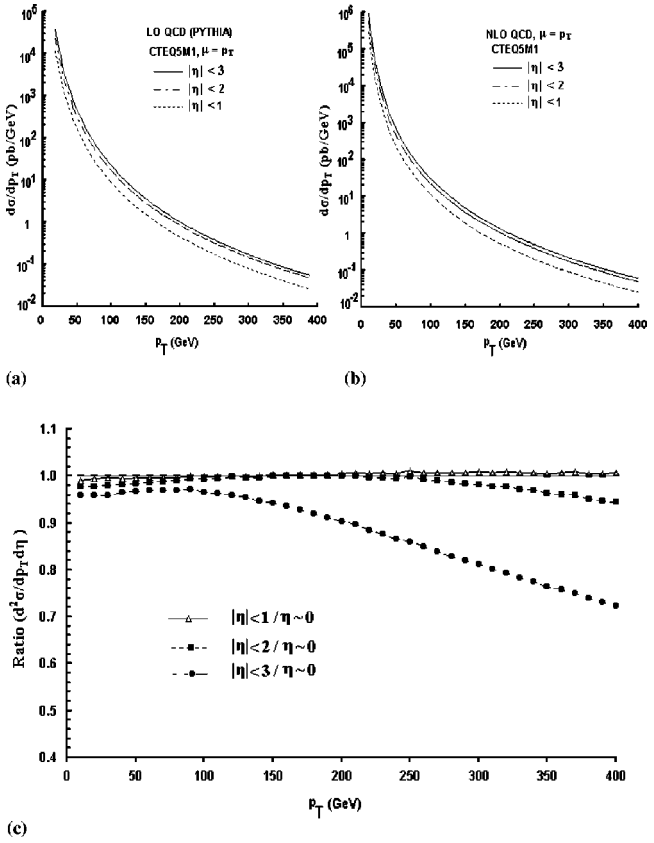

FIG. 9. Pseudorapidity bin size dependence of direct photon cross section at $\sqrt{s}=14$ TeV: (a) NLO QCD predictions with CTEQ5M1 and evaluated at $\mu=p_T$ integrated in different η intervals. (b) Ratio of cross sections in different η bins normalized to that in the central rapidity region.

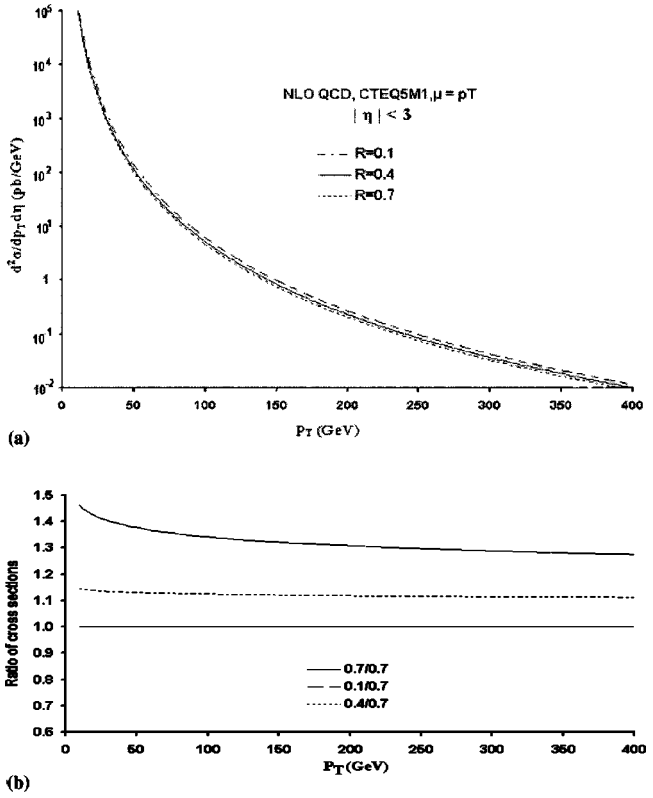

FIG. 10. Cone size dependence of direct photon cross section at $\sqrt{s}=14$ TeV: (a) p_T spectra of NLO QCD predictions for different cone sizes with CTEQ5M1 and evaluated at $\mu=p_T$. (b) Ratio of cross sections for different cone sizes to that of the cross section for 0.7 cone size.

function of p_T in the pseudorapidity bin ($|\eta|<3$) using the CTEQ5M1 parton distribution function and the renormalization scale $\mu=p_T$. Figure 10(b) shows the spectrum of the ratio of cross sections with different cone sizes to that of cone size$=0.7$. As can be seen from the figures, the cross section decreases as cone size increases. At $p_T=50$ GeV, changing the cone size from 0.1 to 0.4 and 0.7 reduces the cross section by 13% and 38%, respectively. This behavior is expected because the isolation criterion excludes events with a certain hadronic energy E_0 inside a cone of size R. Now, keeping E_0 fixed and increasing R means that we are not even allowing such events in a large cone, so it is a stricter criterion (keeping in mind that the jet cross section increases considerably with cone size [47]), and hence the cross section must decrease. We see from Fig. 10(b) that cross section decreases almost uniformly over the whole region except at low p_T for cone size$=0.1$ where it shows some shape dependence.

H. Signal-to-background ratio

The spectrum of signal-to-background ratio [5] for a two jet background is shown in Fig. 11 for the range 20 GeV $<p_T<70$ GeV in the pseudorapidity region $|\eta|<3$. The γ/π^0 ratio rises from around 15% at $p_T=20$ GeV to around 55% at $p_T=60$ GeV and will surpass π^0 production at around 90 GeV.

VII. CONCLUSIONS

Direct photon production continues to be an interesting arena to test perturbative QCD calculations. In this paper, we have compared the isolated prompt photon data measured by CDF at $\sqrt{s}=1.8$ TeV with the NLO predictions using the latest parton distribution function. The results show a clear excess of data over theory for $p_T<25$ GeV. It suggests that a more complete theoretical understanding of processes that contribute to low p_T behavior of the photon cross section is needed which have been addressed by resuming higher order contributions.

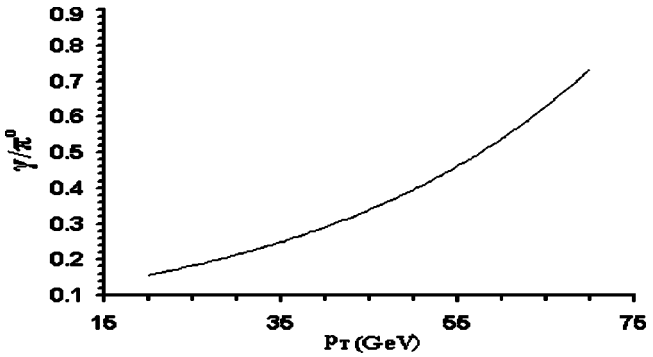

FIG. 11. The p_T spectrum of signal-to-background ratio due to π^0 decay.

The LHC run with greatly extended kinematical range and high statistical precision of data will offer tremendous opportunities to refine our understanding of the production of photons in hard scattering processes. We have presented in detail the study of direct photon rate at the LHC energy. We see that the rate of prompt photon production is very high at LHC compared to that at Tevatron. PYTHIA results indicate that the Compton scattering will dominate the production mechanism in the entire kinematical range considered in the analysis. The p_T spectrum of the relative contributions of LO and NLO cross section shows that the higher order contribution dominates in the low p_T region but decreases in importance considerably at high p_T. The NLO QCD predictions depend only marginally on the choice of renormalization scale. The p_T distribution of direct photon cross section is almost insensitive to the different parametrizations of gluon distributions in the high p_T region ($p_T > 300$ GeV), but shows quite a bit of sensitivity at small p_T values. We also see that at low values of p_T, the shape of the rapidity distribution of the photon cross section is very sensitive to the small-x behavior of gluon distribution. This means that the η spectrum can be used to constrain the gluon distributions. We notice that direct photons are produced fairly copiously in the central rapidity region. Their production cross section depends strongly on the cone size (used in the isolation cut) and is found to decrease with increasing cone size. We have also noted that the γ/π^0 ratio enhances with the rise in p_T and surpasses π^0 production at around 90 GeV.

ACKNOWLEDGMENTS

We are grateful to Werner Vogelsang for his assistance with the NLO theoretical calculations as well as for his consistent encouragement throughout this work. We thank Torbjorn Sjostrand, Steve Kuhlmann, Lenny Apanasevich, and Vishnu Zutshi for some enlightening suggestions related to PYTHIA simulations. We also wish to thank Manjit Kaur, Vipin Bhatnagar, and Dana Partos for useful discussions. Our sincere thanks are to the Department of Science and Technology (DST) for providing the necessary infrastructure. Ashish Kumar, Manoj Kumar Jha, and Kirti Ranjan would also like to express their gratitude to the Council of Scientific and Industrial Research (CSIR) for providing financial assistance.

[1] J.F. Owens, Rev. Mod. Phys. **59**, 465 (1987).
[2] T. Ferbel and W.R. Molzon, Rev. Mod. Phys. **56**, 181 (1984).
[3] W. Vogelsang and M.R. Whally, J. Phys. G **23**, Suppl. 7A (1997).
[4] G. Sterman *et al.*, Rev. Mod. Phys. **67**, 157 (1995).
[5] F. Halzen and D. Scott, Phys. Rev. D **21**, 1320 (1980).
[6] P. Aurenche *et al.*, Phys. Rev. D **42**, 1440 (1990).
[7] P. Aurenche *et al.*, Nucl. Phys. **B399**, 34 (1993).
[8] G. Ballochi *et al.*, Phys. Lett. B **436**, 222 (1998).
[9] M. Begel, Ph.D. thesis, University of Rochester, 1999.
[10] P. Aurenche *et al.*, Nucl. Phys. **B297**, 661 (1988).
[11] L.E. Gordon and W. Vogelsang, Phys. Rev. D **50**, 1901 (1994).
[12] F. Aversa *et al.*, Nucl. Phys. **B327**, 104 (1989).
[13] CTEQ Collaboration, H.L. Lai *et al.*, Phys. Rev. D **55**, 1280 (1997).
[14] A.D. Martin *et al.*, Eur. Phys. J. C **4**, 463 (1998); Nucl. Phys. B (Proc. Suppl.) **79**, 210 (1999).
[15] M. Gluck, E. Reya, and A. Vogt, Eur. Phys. J. C **5**, 461 (1998).
[16] M. Gluck, E. Reya, and A. Vogt, Phys. Rev. D **48**, 116 (1993).
[17] L. Bourhis, M. Fontannaz, and J.Ph. Guillet, Eur. Phys. J. C **2**, 529 (1998).
[18] P.M. Stevenson and H.D. Politzer, Nucl. Phys. **B277**, 756 (1986).
[19] P. Aurenche *et al.*, Phys. Lett. **140B**, 87 (1984).
[20] P. Aurenche *et al.*, Nucl. Phys. **B286**, 553 (1987).
[21] P. Aurenche *et al.*, Nucl. Phys. **B297**, 661 (1988).
[22] P. Aurenche *et al.*, Phys. Rev. D **39**, 3275 (1989).
[23] E.L. Berger and J. Qiu, Phys. Rev. D **44**, 2002 (1991).
[24] P. Aurenche *et al.*, Nucl. Phys. **B399**, 34 (1993).
[25] M. Gluck, L.E. Gordon, E. Reya, and W. Vogelsang, Phys. Rev. Lett. **73**, 388 (1994).
[26] W. Vogelsang and A. Vogt, Nucl. Phys. **B453**, 334 (1995).
[27] H. Baer, J. Ohnemus, and J.F. Owens, Phys. Lett. B **234**, 127 (1990).
[28] H. Baer, J. Ohnemus, and J.F. Owens, Phys. Rev. D **42**, 61 (1990).
[29] H. Weerts *et al.*, Summary Report of the QCD Collider Group, D0 Internal Note, 916, 1989.
[30] T. Sjostrand, L. Lonnblad, and S. Mrenna, hep-ph/0108264, LU TP 01-21, 2001.
[31] D. Acosta *et al.*, Phys. Rev. D **65**, 112003 (2002).
[32] W. Vogelsang (private communications).
[33] CTEQ Collaboration, H.L. Lai *et al.*, Eur. Phys. J. C **12**, 375 (2000).
[34] D. S. Partos, Ph.D. thesis, Brandeis University, 2001.
[35] J. Huston *et al.*, Phys. Rev. D **51**, 6139 (1995).
[36] L. Apanasevich *et al.*, Phys. Rev. Lett. **81**, 2642 (1998).
[37] L. Apanasevich *et al.*, Phys. Rev. D **59**, 074007 (1999).
[38] L. Apanasevich *et al.*, Phys. Rev. D **63**, 014009 (2001).
[39] J. Botts *et al.*, Phys. Lett. B **304**, 159 (1993).
[40] E. Laenen, G. Sterman, and W. Vogelsang, Phys. Rev. Lett. **84**, 4296 (2000).
[41] N. Kidonakis and J.F. Owens, Phys. Rev. D **61**, 094004 (2000).
[42] M. Spira and M. Dittmar, CMS NOTE 1997/080, 6 Oct. 1997.
[43] CTEQ Collaboration, H.L. Lai *et al.*, Phys. Rev. D **51**, 4763 (1995).
[44] CTEQ Collaboration, H.L. Lai *et al.*, Phys. Rev. D **55**, 1280 (1997).
[45] CTEQ Collaboration, J. Huston *et al.*, Phys. Rev. D **58**, 114034 (1998).
[46] M. Gluck, E. Reya, and A. Vogt, Z. Phys. C **67**, 433 (1995).
[47] M. Bhattacharjee, Ph.D. thesis, Delhi University, 1997.